

GENs: Generative Encoding Networks

Surojit Saha Shireen Elhabian Ross T. Whitaker

Scientific Computing and Imaging Institute,
School of Computing, University of Utah, Salt Lake City, UT, USA
surojit@cs.utah.edu, shireen@sci.utah.edu, whitaker@cs.utah.edu

Abstract

Mapping data from and/or onto a known family of distributions has become an important topic in machine learning and data analysis. Deep generative models (e.g., generative adversarial networks) have been used effectively to match known and unknown distributions. Nonetheless, when the form of the target distribution is known, analytical methods are advantageous in providing robust results with provable properties. In this paper, we propose and analyze the use of nonparametric density methods to estimate the Jensen-Shannon divergence for matching unknown data distributions to known target distributions, such as Gaussian or mixtures of Gaussians, in latent spaces. This analytical method has several advantages: better behavior when training sample quantity is low, provable convergence properties, and relatively few parameters, which can be derived analytically. Using the proposed method, we enforce the latent representation of an autoencoder to match a target distribution in a learning framework that we call a *generative encoding network*. Here, we present the numerical methods; derive the expected distribution of the data in the latent space; evaluate the properties of the latent space, sample reconstruction, and generated samples; show the advantages over the adversarial counterpart; and demonstrate the application of the method in real world.

1 Introduction

Research in statistical modeling and deep learning has made great strides in the discovery of latent spaces in the context of nonlinear, high-dimensional, and very general transformations, such as those developed by autoencoders that employ deep neural networks (Tschannen et al., 2018). Meanwhile, there have also been significant advances in generative models, which can systematically produce data samples from complex, high-dimensional distributions that resemble populations of training data. While encoder technologies, such as deterministic denoising (Vincent et al., 2008) and contractive (Rifai et al., 2011) autoencoders, can produce latent representation for samples, the structure of the population of data in that latent space is often

underspecified or unconstrained, such that one cannot readily reason about that distribution or sample from them. Thus, such models often fail as generators of new samples. Generators on the other hand, such as those produced by the generative adversarial network (GAN) (Goodfellow et al., 2014), have demonstrated impressive capabilities to produce new, very realistic samples (both qualitatively and quantitatively) from complex distributions described by training data. This is achieved, typically, by learning a transformation from a known distribution in a latent space into the high-dimensional data space. However, the inverse mapping is often problematic (from samples into the latent space), and therefore it is often difficult to reason about the absolute or relative positions of data in that latent space. Models that map training samples into latent spaces with well-defined properties are of significant value and interest. For instance, using such mappings, one could compute data densities in the latent space, and alleviate some of the challenges of density estimation of arbitrary distributions in high-dimensional spaces. This could be relevant for unsupervised learning methods, such as anomaly detection (Chalapathy and Chawla, 2019). One might also want to compare or manipulate data samples in the latent space, and thereby generate new, realistic samples in controlled ways (Zhu et al., 2016). These motivations, and others, have led to more recent research that seeks to build latent spaces that have two properties (i) an approximate invertible mapping from the data space to the latent space and (ii) data in the latent space has defined statistical characteristics that lead to probabilistic reasoning and sample generation. These developments and motivations have led to several novel architectures that attempt to unify latent-space learning and sample generation. Of particular interest for this work are the methods that structure the distribution of data in the latent space of an autoencoder. Very promising results, for instance, have been demonstrated by the adversarial autoencoders (AAE) of Makhzani et al. (Makhzani et al., 2016), where a conventional autoencoder incurs an additional penalty from a discriminator in the latent space, which compares (via classification) the latent

encodings of training samples to samples from a known distribution (e.g., standard normal).

In this paper, we take an alternative approach. Rather than using an adversary to compare distributions, we propose a nonadversarial framework, *generative encoding networks* or GENs, to enforce the latent representation of an autoencoder to a known target distribution. We penalize distributions in the latent space directly using the Jensen-Shannon divergence (JSD) of the distribution of the encoded training data and the known distribution. The density of the encoded training data is estimated with a kernel density estimator (KDE) and we compare against (match to) analytical distributions. The important insight is that known distributions, such as the standard normal, in spaces of relatively low dimension (compared to the data space) lend themselves to accurate estimates with KDEs and facilitate the automatic estimation of auxiliary or hyper-parameters, such as kernel bandwidth. GENs have several advantages. First, they avoid the complexity of solving the min-max optimization problem with competing networks, which can present challenges in choices of architecture and training strategies/parameters. Second, we show that there are scenarios where the use of KDE-based JSD is a more accurate measure of the difference between two different distributions compared with the estimates of a corresponding adversary. Finally, the use of analytical tools allows us to reason about (or predict) the parameters and behavior of the system in ways that are not readily available with a conventional adversarial neural network.

2 Related Work

Directly related to GENs are deep, generative models that build low-dimensional latent spaces with known/quantifiable properties (e.g., known density such as multivariate normal) and learn a functional mapping from this latent space to the data space. Variational autoencoders (VAEs) (Kingma and Welling, 2014; Rezende et al., 2014) introduce a parametric prior distribution on the latent space and learns an inference network (i.e., encoder) jointly with the generative model (i.e., decoder) to maximize a variational lower bound of the otherwise intractable marginal log-likelihood of the training data. Nonetheless, VAEs often fail to match the marginal (a.k.a. aggregate) posterior to the latent prior distribution, manifested by poor sample quality (Rosca et al., 2018). VAE variants, such as adversarial (Makhzani et al., 2016) and Wasserstein (Tolstikhin et al., 2017) autoencoders, introduce structure to the aggregate posterior distribution to match the latent distribution through matching penalties (adversarial or maximum mean discrepancy, MMD, regularizers) in the latent space, which, in the

limit, optimize the Jensen-Shannon divergence (JSD) of the different distributions. Other VAE variants improve matching distributions in the latent space through learning a data-driven prior distribution using normalizing flows in the low-dimensional latent space (Bhalodia et al., 2019; Xiao et al., 2019). To mitigate vanishing gradients in GANs (Arjovsky and Bottou, 2017), KernelGANs (Sinn and Rawat, 2018) use a training objective that minimizes a nonparametric estimate of the JSD in the data space. However, such estimates in very high-dimensional spaces, where the data often lies, pose theoretical and computational challenges (Theis et al., 2015; Wu et al., 2017), for instance, the estimation of the kernel bandwidth. GANs, in their basic form (Goodfellow et al., 2014), do not provide reliable mappings back into the latent space. Encoder-decoder GAN variants (e.g., BiGAN (Donahue et al., 2017), ALI (Dumoulin et al., 2017)) simultaneously learn inference and generator networks. However, reconstructed samples from their latent representation do not preserve sample identity since the data-latent correspondence is learned through a discriminator that approximates a density ratio between their joint distribution. Several works have introduced different GAN and autoencoder hybrids that bring the best of both worlds—generating realistic samples and approximately/softly invertible architectures (Rosca et al., 2017). For instance, adversarial generator-encoder (AGE) (Ulyanov et al., 2018) trains an encoder and a generator in opposite directions by considering the divergence of both the encoded real data and encoded generated data to the latent prior distribution. Distributions are matched using KL divergence by empirically fitting a multivariate Gaussian with a diagonal covariance to the encoded data.

3 Generative Encoding Networks

GENs augment the loss function of a conventional autoencoder with a term that penalizes the difference between distribution of training samples in the latent space (i.e., *encoded* distribution) and the desired or *target* distribution. We denote the distribution of training data, in the space in which it was given (i.e., data space) as $p(\mathbf{x})$ with $\mathbf{x} \in \mathbb{R}^d$, the distribution of *encoded* training data in the latent space as $p_e(\mathbf{z})$ with $\mathbf{z} \in \mathbb{R}^l$, and the *target* distribution in the latent space as $p_t(\mathbf{z})$. Let $\mathbf{x}_1, \dots, \mathbf{x}_n$ and $\mathbf{z}_1, \dots, \mathbf{z}_n$ be the n -training samples and associated latent space representations, respectively, such that $\mathbf{z}_i = E_\phi(\mathbf{x}_i)$, where ϕ denotes the network parameters of the encoder.

For penalizing the difference between p_e and p_t , we use the Jensen-Shannon divergence. This penalty has the advantages of being a true metric with respect to the two distributions and having values between 0 and 1 (in the analytical case), which controls the influence

of the penalty under a wide range of circumstances. However, while the expectation can be approximated with a sample mean, it requires an estimate of the ratios of probabilities, which typically require density estimates and can be challenging.

Makhzani et al. (Makhzani et al., 2016), in the context of GANs, note that an ideal discriminator *adversary* classifying samples between p_t and p_e with a cross entropy loss, computes the ratio of densities required for the divergence and the cross entropy is proportional to the JSD $[p_t, p_e]$. This is a very powerful result, but requires the design and training of a discriminator that can approximate the ideal one, with the associated hyper-parameters, architectural choices, and training strategies. In this work, we rely on the following observation: *in cases where the p_t has a known regular form, which it often does, we can rely on this form to compute good approximations to p_e through samples, without the need of an additional neural network, or adversary.*

In principle, the target distribution, $p_t(\mathbf{z})$ of a GEN, can be *any distribution* from which we can sample, but in this paper we focus on the cases where the target distribution is Gaussian or Mixture of Gaussians, and we propose a kernel density estimate (KDE) of p_e from a set of m -samples $\mathbf{z}_1, \dots, \mathbf{z}_m$, such that:

$$p_e(\mathbf{z}) = \frac{1}{m} \sum_{i=1}^m K\left(\frac{\|\mathbf{z} - \mathbf{z}_i\|}{h}\right) \quad (1)$$

where $h \in \mathbb{R}^+$ denotes the kernel bandwidth. Without loss of generality, we consider isotropic Gaussian kernels, and denote it as $G_h(\mathbf{z} - \mathbf{z}_i)$.

Under these conditions, the KDE-based JSD loss is as follows (leaving out constants):

$$\begin{aligned} \text{JSD}[p_e, p_t] = & \mathbb{E}_{\mathbf{z}' \sim p_e(\mathbf{z})} \left\{ \log \left[\frac{\frac{1}{m} \sum_{i=1}^m G_h(\mathbf{z}' - \mathbf{z}_i)}{p_t(\mathbf{z}') + \frac{1}{m} \sum_{i=1}^m G_h(\mathbf{z}' - \mathbf{z}_i)} \right] \right\} \\ & + \mathbb{E}_{\mathbf{z}'' \sim \mathcal{N}(\mathbf{0}, \mathbf{I})} \left\{ \log \left[\frac{p_t(\mathbf{z}'')}{p_t(\mathbf{z}'') + \frac{1}{m} \sum_{i=1}^m G_h(\mathbf{z}'' - \mathbf{z}_i)} \right] \right\} \end{aligned} \quad (2)$$

Notice there are *three* sets of samples from the latent space in (2), denoted \mathbf{z} , \mathbf{z}' , and \mathbf{z}'' . The first set, \mathbf{z} , of size m , are the samples used to build the KDE of p_e as in (1). The second set, \mathbf{z}' from p_e are used to compute the sample mean (approximating the expectation) of the log term containing the ratio $p_e/(p_e + p_t)$. The third set, \mathbf{z}'' , are the samples from the target distribution (which can be generated analytically) that are used to compute the expectation, via the sample mean, of $p_t/(p_e + p_t)$. The choices of these three sets

present some engineering decisions and how we construct derivatives and update the model.

In this work, we propose to let the samples \mathbf{z} for the KDE represent the overall state of the encoder network E , with sufficient samples from the training data, and to let that set lag the updates of the autoencoder, much as we would do with an adversarial network. The expectation in the first term of (2), over the samples \mathbf{z}' , are used to compute the gradient, and that set comprises the *minibatch* (i.e., sampled from the training data), which allows us to train the encoder using stochastic gradient descent. In this case, the second term in (2) does not affect the update of the autoencoder, and can be ignored.

This strategy leaves us with two important decisions regarding hyper-parameters. The first is the choice of number of samples m to be used in the lagging, KDE-based estimate of p_e and the second is the bandwidth h used in that same estimate. Of course, bandwidth selection for KDE is, in general, a very challenging problem without a completely satisfying, general solution. However, because we are quantifying differences with target distributions, where accuracy is most important when distributions are similar, we can use the target distribution itself, the dimensionality of the latent space, l , and the size of the sample set used in the KDE (m above) to estimate the optimal bandwidth, h_{opt} . We seek the h_{opt} that best differentiates two sample sets, and therefore maximizes the JSD between two sample sets from the target distribution.

Given only a dimension and a number of samples for the KDE estimate, we can estimate the optimal bandwidth by either root trapping or a fixed-point method on h , by evaluating the derivative of (2) with respect to h , that is $\partial \text{JSD}[p_e, p_t] / \partial h$. For target distribution as standard normal, Table 1 shows the optimal bandwidth estimates for a variety of latent dimensions, l , and number of samples, m . As expected, the bandwidth increases with higher dimension and fewer samples.

The loss function of GENs can thus be formulated as,

$$\begin{aligned} \mathbb{E}_{\mathbf{x} \sim p(\mathbf{x})} \left\{ \|\mathbf{x} - D_\theta(E_\phi(\mathbf{x}))\|_2^2 \right\} + & \quad (3) \\ \mathbb{E}_{\mathbf{x} \sim p(\mathbf{x})} \left\{ \lambda \log \left[\frac{\frac{1}{m} \sum_{i=1}^m G_h(E_\phi(\mathbf{x}) - \mathbf{z}_i)}{p_t(E_\phi(\mathbf{x})) + \frac{1}{m} \sum_{i=1}^m G_h(E_\phi(\mathbf{x}) - \mathbf{z}_i)} \right] \right\} \end{aligned}$$

Algorithm 1 : GENs training. Minibatch stochastic gradient descent of GENs loss (3).

Input: Training samples $\mathcal{X} = \{\mathbf{x}_1, \dots, \mathbf{x}_n\}$, Minibatch size n_b , Latent dimension l , Number of lagged samples for KDE m , Number of minibatch updates the KDE estimate should lag k_b , Relative scaling factor for the JSD loss λ

Output: encoder parameters ϕ and decoder parameters θ

- 1: Estimate the optimal kernel bandwidth h_{opt} given (l, m)
- 2: Initialize ϕ and θ
- 3: Initialize lagging samples for KDE $\mathcal{Z} \subset \{E_\phi(\mathbf{x}_1), \dots, E_\phi(\mathbf{x}_n)\}$, where $|\mathcal{Z}| = m$
- 4: Initialize minibatch index $b \leftarrow 0$
- 5: **for** number of minibatch updates **do**
- 6: Sample a minibatch of size n_b from $p(\mathbf{x})$, $\mathcal{X}_b = \{\mathbf{x}_1, \dots, \mathbf{x}_{n_b}\}$
- 7: Encode minibatch samples in the latent space $\mathcal{Z}'_b = \{\mathbf{z}'_1, \dots, \mathbf{z}'_{n_b}\}$, where $\mathbf{z}'_i = E_\phi(\mathbf{x}_i)$
- 8: Update the encoder parameters, ϕ using stochastic gradient descent:

9:

$$\nabla_\phi \frac{1}{n_b} \sum_{i=1}^{n_b} \left\{ \|\mathbf{x}_i - D_\theta(E_\phi(\mathbf{x}_i))\|_2^2 \right\} + \lambda \nabla_\phi \frac{1}{n_b} \sum_{i=1}^{n_b} \left\{ \log \frac{\frac{1}{m} \sum_{i=1}^m G_h(\mathbf{z}' - \mathbf{z}_i)}{p_t(\mathbf{z}') + \frac{1}{m} \sum_{i=1}^m G_h(\mathbf{z}' - \mathbf{z}_i)} \right\}$$

- 10: Update the decoder parameters, θ using stochastic gradient descent:

11:

$$\nabla_\theta \frac{1}{n_b} \sum_{i=1}^{n_b} \|\mathbf{x}_i - D_\theta(E_\phi(\mathbf{x}_i))\|_2^2$$

- 12: **if** $b \bmod k_b$ **then**

- 13: Update the lagging samples for KDE $\{\mathbf{z}_1, \dots, \mathbf{z}_m\}$, where $\mathbf{z}_i = E_\phi(\mathbf{x}_i)$ using the current state of the encoder

- 14: **end if**

- 15: $b \leftarrow b + 1$

- 16: **end for**
-

where E_ϕ and D_θ are the encoder and decoder with parameters ϕ and θ , respectively. GENs simultaneously updates the encoder E_ϕ , and the decoder D_θ to minimize the expected reconstruction loss in data space \mathbb{R}^d and JSD in latent space \mathbb{R}^l (using KDE of the encoded distribution). Algorithm 1 outlines GENs training. Here, we see the relationship with several other methods. The KDE estimate of JSD acts very much like an adversary. Its single parameter, bandwidth is cho-

sen to maximize the discrimination (also similar to an adversary) between samples from same distributions (i.e. pessimistic assumptions). Furthermore, minimization of JSD loss (by updating the encoder parameters), set up a min-max game as in AAE—except that we know the optimal/final value of the single parameter, bandwidth, in the latent space. There is also a relationship with the VAE formulation. The aggregate latent distribution is a convolution of data samples with a kernel. The difference is that the width of that kernel is chosen specifically to aid analysis in the latent space, rather than basing it on a hypothetical noise model. Furthermore, the JSD penalty directly operates on the aggregate latent distribution, rather than individual samples, as the standard-normal prior does in the VAE. As the results section demonstrate, this results in latent distributions that are better matched to the target.

4 Latent space distribution

The use of analytical approach in the proposed method allows us to determine the resultant distribution in the latent space when the training of the model reaches a steady state, i.e., when the GEN successfully matches the encoded distribution, p_e , to the defined target distribution, p_t . Here, we derived the closed form expression of the resultant distribution in the latent space when the target distribution is standard normal (these results can be generalized to any multivariate Gaussian but is beyond the scope of this paper). When the training of GEN converges, the derivative of the JSD estimate with respect to the training samples \mathbf{z}' approaches zero and the parameters of the encoder, ϕ , are no longer updated. Thus, setting $\partial \text{JSD}[p_e, p_t] / \partial \mathbf{z}'$ to 0 and rearranging the expression we get,

$$\mathbf{z}' \sum_{i=1}^m G_h(\mathbf{z}' - \mathbf{z}_i) = \left(\frac{1}{h^2} \left[\sum_{i=1}^m G_h(\mathbf{z}' - \mathbf{z}_i) (\mathbf{z}' - \mathbf{z}_i) \right] \right) \quad (4)$$

The expression in (4) should hold for every \mathbf{z}' in the latent space, and therefore constrains the configurations of \mathbf{z}_i 's. Because the \mathbf{z}_i 's are stochastic (samples from held out data), we can constrain their probability distribution by taking an expectation on both sides of (4):

$$\mathbb{E}_{\mathbf{z}' \sim p(\mathbf{z}_1, \mathbf{z}_2, \dots, \mathbf{z}_m)} \left\{ \mathbf{z}' \sum_{i=1}^m G_h(\mathbf{z}' - \mathbf{z}_i) \right\} = \mathbb{E}_{\mathbf{z}' \sim p(\mathbf{z}_1, \mathbf{z}_2, \dots, \mathbf{z}_m)} \left\{ \frac{1}{h^2} \left[\sum_{i=1}^m G_h(\mathbf{z}' - \mathbf{z}_i) (\mathbf{z}' - \mathbf{z}_i) \right] \right\} \quad (5)$$

The \mathbf{z}_i 's are independent (e.g., held out samples from the data space) and thus, we can marginalize the inde-

Table 1: Optimal bandwidths, h_{opt} , estimated to maximize the JSD between two standard-normal samples sets. Error bars are computed over 10 trials. Notice that the bandwidth increases with increasing dimensions (vertical) or decreasing sample size (horizontal).

$l \setminus m$	250	500	1000	2000	4000	8000
2	0.46 ± 0.08	0.41 ± 0.04	0.38 ± 0.03	0.34 ± 0.02	0.31 ± 0.03	0.28 ± 0.01
5	0.65 ± 0.03	0.59 ± 0.02	0.55 ± 0.02	0.51 ± 0.01	0.47 ± 0.01	0.44 ± 0.01
10	0.77 ± 0.02	0.73 ± 0.01	0.69 ± 0.01	0.66 ± 0.01	0.63 ± 0.01	0.6 ± 0.01
20	0.92 ± 0.01	0.89 ± 0.01	0.86 ± 0.00	0.82 ± 0.01	0.80 ± 0.00	0.77 ± 0.00
40	> 1.0	> 1.0	> 1.0	0.98 ± 0.00	0.95 ± 0.00	0.94 ± 0.00

pendent variables in (5) and use the linear property of summation to get,

$$\mathbf{z}' \int_{\mathbf{z}_i} G_h(\mathbf{z}' - \mathbf{z}_i) p(\mathbf{z}_i) d\mathbf{z}_i = \frac{1}{(h^2)} \int_{\mathbf{z}_i} G_h(\mathbf{z}' - \mathbf{z}_i) (\mathbf{z}' - \mathbf{z}_i) p(\mathbf{z}_i) d\mathbf{z}_i. \quad (6)$$

The RHS of (6) is the expectation of $\nabla_{\mathbf{z}'} G_h(\mathbf{z}' - \mathbf{z}_i)$. By the definition of convolution and its properties we get,

$$\begin{aligned} \mathbf{z}' [G_h(\mathbf{z}') \otimes p(\mathbf{z}')] &= -\nabla_{\mathbf{z}'} [G_h(\mathbf{z}') \otimes p(\mathbf{z}')] \\ Q(\mathbf{z}') &= [G_h(\mathbf{z}') \otimes p(\mathbf{z}')] \\ \nabla_{\mathbf{z}'} Q(\mathbf{z}') &= -\mathbf{z}' Q(\mathbf{z}') \end{aligned} \quad (7)$$

This is a partial differential equation in (7) with the solution (assuming appropriate boundary/limiting conditions)

$$Q(\mathbf{z}') = k * \exp(-\|\mathbf{z}'\|^2/2) \quad (8)$$

Thus, $p(\mathbf{z}') = G_\sigma(\mathbf{z}')$ where $\sigma^2 = 1 - h^2$. The factor h^2 in the variance of $p(\mathbf{z}')$ accounts for the bias produced by the convolution of samples used in the KDE with the kernel. Note that for a standard-normal target distribution, the distribution of samples in the latent space as the encoder converges will degenerate (to a dirac delta function) as $h \rightarrow 1$. This provides a practical interpretation of Table 1, because as h_{opt} in that table goes to 1, we see the lower bound on the number of samples that would be required for this method to function in any particular latent dimension. For instance, 8000 samples would be barely enough to estimate the JSD between samples from standard normal distributions in $l = 40$ dimensions. This limitation in samples/dimensions is a consequence of our choice of a stationary, isotropic kernel, which suggests that the method could be further improved by the application of nonstationary KDE methods.

5 Results

Here we present some results that demonstrate, empirically the power of the KDE-based approach, relative to a NN adversary, to estimate JSD. We also quantify the

improvement of the latent-space distribution on benchmark dataset while also comparing, qualitatively and quantitatively, the generative properties of related approaches on several datasets. Finally, we demonstrate some potential applications of the method.

5.1 Correlation Study

Here, we compared the proposed KDE-based JSD estimates with the estimates from an adversarial (i.e., discriminator) neural network (NN). We create a set of experiments that control the degree of divergence between two distributions and quantify the ability of these methods to find the correlation between JSD and the parameter that controls these differences. In an ideal scenario, the computed JSD should increase with the parameter that controls the distributions' separation.

For this particular set of experiments, we whiten all datasets, to avoid trivial differences in data, and we compare all manufactured distributions with the standard normal. We construct sequences of distributions (proxies for a hypothetical latent distribution) by a mixture of two standard-normal distributions, separated by distance s and subsequently whitened. The parameter s ranges from 0 to 6. The top of Figure 1 shows examples from these distributions (in 2D) with $s = [0, 3, 6]$. This arrangement allows us to study the behavior of these different methods over multiple trials, different dimensions, l , and different training sample sizes, m .

The single parameter, the bandwidth, for the GEN is computed using the optimization described in Section 3. The NN-discriminator has three hidden layers, with the number of units at each layer proportional to l , and the first layer being the widest, with $10 \times l$ units, and it was regularized using an early stopping criteria which evaluated held-out data.

The middle panel of Figure 1 shows a graph of a particular experiment, $l = 5$ and $m = 1000$, the estimated JSD as a function of s , with error bars showing over 20 trials. The KDE shows an upward trend, while the NN was unable to detect the progressive increase in differences. These slopes and the corresponding error

bars are important, because the derivatives of the JSD estimates are what drive the structure of the latent space in this autoencoder context.

Using this method we can quantify the slope/noise relationship for each method as a function of dimension and sample size. The lower panel of Figure 1 reports the Pearson correlations over a range of dimensions and sample sizes. In each cell, the NN|KDE are on the left|right, respectively. Numbers in bold indicate higher correlations that are statistically significant. These results demonstrate that the estimation of JSD using NN is strongly influenced by sample size and data dimension. In many cases, the KDE is able to quantify correlation where the NN does not.

5.2 Evaluating structure in learned latent spaces

Here we quantify how well-formed the Gaussian structure is in the latent space after the autoencoder is optimized. We rely on the fact that for a given covariance, Σ , the Gaussian has the maximum entropy among all distributions with the same covariance. Thus, we can compute the entropy, $H[p_e]$, of the whitened latent distributions from various learned models to evaluate the *normality* of the encoded distribution for different methods. Evaluating entropy relies on estimates of density. For this, we also use a KDE, as defined in (1). For a certain latent dimension l , and sample size m , the optimal bandwidth h_{opt} can be determined by minimizing the entropy of the KDE estimate of a distribution given samples from it (maximum log likelihood). This is in contrast to estimating the bandwidth using JSD that best differentiates two distributions, encoded and target. To find h_{opt} that minimizes the entropy of a set of latent space samples, we differentiate $H[p_e]$ with respect to h , set it equal to zero, and solve for h_{opt} with a fixed point strategy. We have,

$$H[p_e(\mathbf{z})] \approx -\frac{1}{m} \sum_i \log \frac{1}{m-1} \sum_{j \neq i} K \left(\frac{\|\mathbf{z}_j - \mathbf{z}_i\|}{h} \right), \quad (9)$$

We evaluate the entropy of the latent distributions for the proposed GEN, AAE(Makhzani et al., 2016) and VAE (Kingma and Welling, 2014) for varying training sample sizes. If the latent representation closely matches the targeted, standard-normal distribution, then its entropy will match that of standard normal for that dimension, which has analytical expression. For a fair comparison, the architecture of the E_ϕ and D_θ used is same for all the methods. For this experiment, we have used only fully connected (FC) layers, and henceforth we refer to this architecture as *FC-layers*. For statistical evaluation, we have trained 5 different models of the network for each method for

different settings. This experiment is conducted on MNIST data set with latent dimension of $l = 8$. Table 2, shows that the entropy of GEN is consistently higher than that of AAE and VAE for all the sample sizes and almost equal to the entropy estimated for samples drawn from standard-normal distribution using the same numerical methods. The true entropy of the standard normal distribution with $l = 8$ is 11.35, very close to our numerical estimates and that of the GEN. The observation for VAE is consistent with (Rosca et al., 2018). For the data reported in Table 2, the reconstruction losses of GEN, AAE(Makhzani et al., 2016) and VAE(Kingma and Welling, 2014) for all sample sizes were observed to be approximately 0.02, close to the loss of unconstrained autoencoder, ruling that out as a confounding factor in the reported differences.

5.3 Training of GENs on bench-mark data

We examine qualitative results for several benchmark datasets: MNIST, CelebA and SVHN, with a standard-normal target. For training GEN, we use a subset of the training data for the lagging samples of the KDE-estimate. This size, m , is set to 20K for CelebA and 10K for MNIST and SVHN. The latent dimensions, l , are 8, 25 and 40 for MNIST, SVHN and CelebA respectively. The relative scaling factor λ , for JSD loss was in the range $[0.01, 0.005]$ for different scenarios. In all our experiments, we have used Adam optimizer (learning rate: $2e^{-04}$, β_1 : 0.5). Number of minibatch updates the KDE estimate should lag, k_b , is set to 10. The FID score of GEN and other competing methods for different datasets are reported in Table 3. Qualitative results of the different methods trained over CelebA dataset are shown in Figure 2. Quantitative results show that the GEN generates marginally better data-space examples than AAE and VAE. This can be confirmed, qualitatively, by the generated samples in Figure 2.

5.4 Semi-supervised learning

In this experiment, we model the distribution in the latent space as mixture of Gaussians (MoG) distributions where each mode in the mixture corresponds to a category of input data, similar to the results in (Makhzani et al., 2016). To map input data to a specific mode of the distribution (depending on its category), we have used the labels of the data for a small set of examples. The idea is to leverage these partially labeled examples to map unlabeled data to its corresponding mode. This experiment was designed on MNIST dataset for the target distribution as the mixture of 10 Gaussians where each mode represents different digit $[0 - 9]$. For training, we have used 10K labeled samples, and 40K unlabeled. For the KDE estimate of the encoded distri-

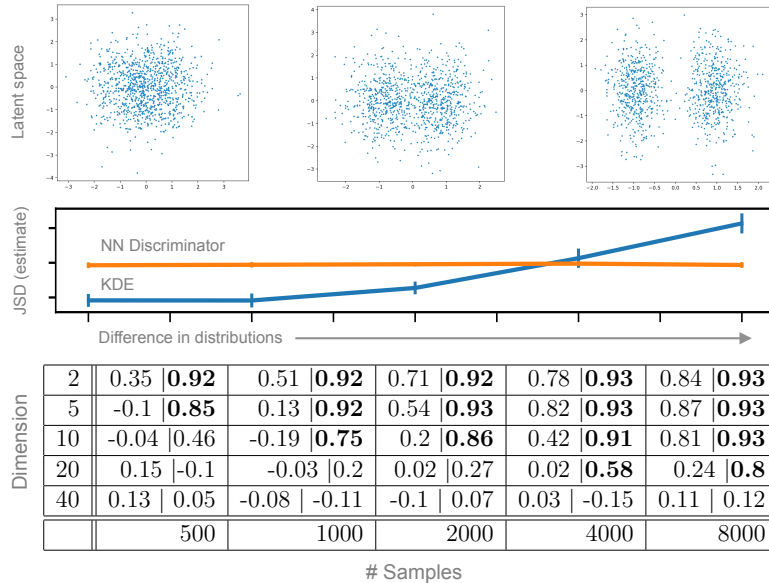


Figure 1: Top: Sequences of distributions, all with the same variance, that differ in controlled ways from the target (standard normal) allow us to evaluate a methods ability to quantify these differences. A line graph with error bars shows how a neural network (NN) and a kernel density estimator (KDE) estimate of JSD for different degrees of separation of the underlying distributions (as above) for 5 dimensions and 1000 samples. Bottom: Comparing distributions with varying degrees of separation (numerous trials) gives Pearson correlation coefficients for NN (left of bars) and KDE for varying dimensions and numbers of samples. Bold indicates significant correlations that are higher than the alternative model.

Table 2: Mean and standard deviation of entropy of the latent representations generated with AAE (Makhzani et al., 2016), VAE (Kingma and Welling, 2014) and GEN using the *FC-layers* architecture over MNIST data set with latent dimension of $l = 8$.

Method \ Samples	1000	2000	5000	10000
AAE	6.552 ± 1.8164	8.408 ± 0.5280	8.742 ± 0.4209	9.862 ± 1.1321
VAE	10.478 ± 0.1647	10.483 ± 0.2013	10.347 ± 0.0769	10.130 ± 0.1516
GEN (proposed)	11.681 ± 0.0231	11.622 ± 0.0170	11.497 ± 0.0068	11.464 ± 0.0036
Standard Normal	11.668 ± 0.0552	11.621 ± 0.0597	11.575 ± 0.0200	11.538 ± 0.0162

Table 3: FID score of competing methods for different datasets (lower is better)

	AAE	VAE	GEN
SVHN	56.08 ± 0.35	55.21 ± 0.24	45.52 ± 0.33
CelebA	52.65 ± 0.06	55.51 ± 0.25	43.65 ± 0.09

bution, p_e , we have used $m = 10K$ samples, separate from the training data. The optimum bandwidth for KDE, h_{opt} , is determined by using samples from the target distribution (MoG) such that it maximizes the JSD between two sample sets from the target distribution. Projection of the held out data in the latent space using a trained model is shown in Figure 3, demonstrating that the GEN maps the test inputs to the correct mode.

5.5 Novelty detection

Novelty detection is the method of detecting the rare events or outliers relative to the prevalent samples (aka inliers). Most of the methods for outlier detection, using the encoder-decoder architecture, relies on the reconstruction loss (Xia et al., 2015) or the employs a one-class classifier (Sabokrou et al., 2018) to predict outliers. Here, we detect anomaly using the estimated probability in the data space, which is similar in philosophy to (Pidhorskyi et al., 2018), but we present a very different mathematical formulation. Strictly invertible networks (Dinh et al., 2017) can estimate data density using latent space density and transformation Jacobians. In the encoder-decoder architecture of an autoencoder, we must account for the lower dimension of the model in the data space. Thus, we construct the probability in the data space using the in-manifold

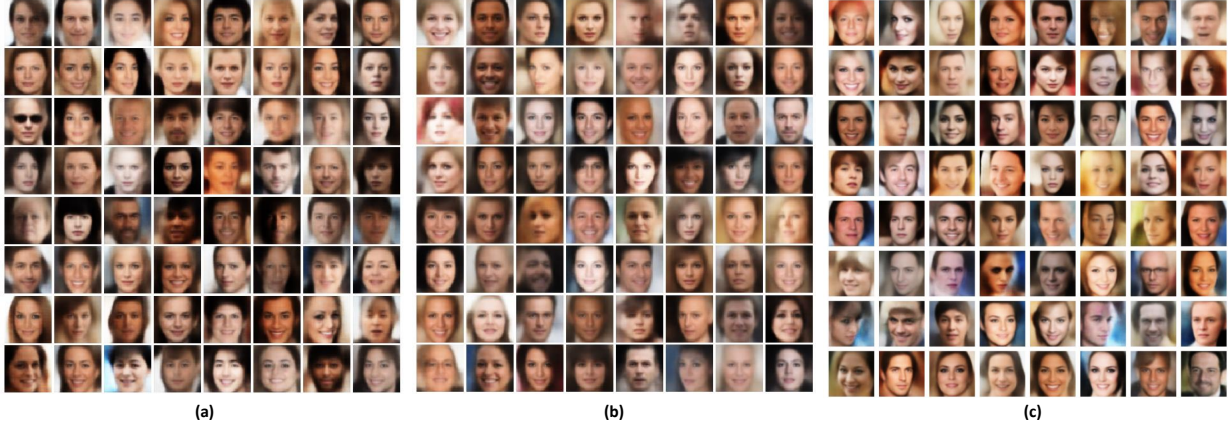


Figure 2: Generated images for CelebA dataset in $l = 40$ dimensional latent space for different methods, (a) AAE (Makhzani et al., 2016) (b) VAE (Kingma and Welling, 2014) and (c) GEN (proposed)

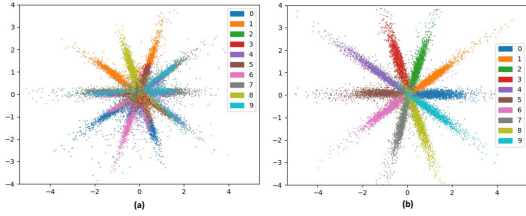


Figure 3: Mapping of MNIST to 10 2D Gaussians in the latent space (a) without any supervision (b) with labels for 10K samples.

probability (manifold of dimension l projected from the latent to data space, parameterized by the probability in the latent space and Jacobian of the mapping) and off-manifold probability (projection of sample on the manifold in data space). Probability in the data space is thus computed as follows:

$$p(\mathbf{x}) = p(\mathbf{z}') \left| \det \frac{\partial \mathbf{x}'}{\partial \mathbf{z}'} \right|^{-1} p(\mathbf{x}|\mathbf{x}') \quad (10)$$

Where, $\mathbf{z}' = E_\phi(\mathbf{x})$ and $\mathbf{x}' = D_\theta(E_\phi(\mathbf{x}))$

$p(\mathbf{z}') \left| \det \frac{\partial \mathbf{x}'}{\partial \mathbf{z}'} \right|^{-1}$ is the in-manifold probability

$p(\mathbf{x}|\mathbf{x}') = \mathcal{N}(\mathbf{x}; \mathbf{x}', \sigma^2 \mathbf{I})$ is the off-manifold probability

For the effects of change of coordinates, we use the first fundamental form to compute $\det \frac{\partial \mathbf{x}'}{\partial \mathbf{z}'}$ as,

$$\text{Let } \mathbf{A} = \frac{\partial \mathbf{x}'}{\partial \mathbf{z}'} \text{ and } \mathbf{B} = \mathbf{A}^T \mathbf{A} \text{ then, } \det \mathbf{A} = \sqrt{|\det \mathbf{B}|} \quad (11)$$

This outlier detection method is applied over the MNIST dataset and the results are shown in Figure 4. In this experiment, outlier prediction is done for individual category of digits in the held out data. The outlier score for a test sample is computed as the negative log of the probability in the data space. We have shown the 100 highest and lowest probability test sam-

ples, sorted by the outlier scores, in Figure 4. The first 100 samples with low score are considered inliers to the distribution, while the last 100 are identified as outliers, which possibly belong to the low probability region.

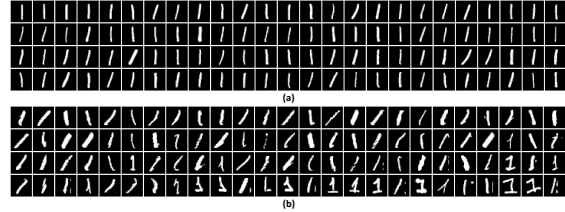


Figure 4: Novelty detection on the held out data of MNIST for digit 1 (a) 100 samples with low outlier score aka inliers and (b) 100 samples having high outlier score, identified as outliers to the distribution

6 Discussion

The proposed GEN method is very promising in its ability to generate latent space representations that adhere to target distributions and associated generative models. The method has fewer parameters than alternatives and produces results that compare favorably with previous methods in terms of both the latent space structure and the generated data. One important remaining challenge is dimensionality. While we report results for $l = 40$, the method starts to break down above $l = 50$, where optimal bandwidths are too high for virtually any number of samples and KDE-estimates with stationary kernels become impractical. This is, of course, the classic curse of dimensionality, which any method that attempts to compute statistics in such spaces faces. However, the method could almost certainly be pushed into somewhat high dimensions using more sophisticated KDE methods—one area of further investigation.

References

- M. Arjovsky and L. Bottou. Towards principled methods for training generative adversarial networks. *arXiv preprint arXiv:1701.04862*, 2017.
- R. Bhalodia, I. Lee, and S. Elhabian. dpvae: Fixing sample generation for regularized vaes. *arXiv preprint arXiv:1911.10506*, 2019.
- R. Chalapathy and S. Chawla. Deep learning for anomaly detection: A survey. *arXiv preprint arXiv:1901.03407*, 2019.
- L. Dinh, J. Sohl-Dickstein, and S. Bengio. Density estimation using real nvp. *International Conference on Learning Representations (ICLR)*, 2017.
- J. Donahue, P. Krähenbühl, and T. Darrell. Adversarial feature learning. *International Conference on Learning Features (ICLR)*, 2017.
- V. Dumoulin, I. Belghazi, B. Poole, O. Mastropietro, A. Lamb, M. Arjovsky, and A. Courville. Adversarially learned inference. *International Conference on Learning Features (ICLR)*, 2017.
- I. Goodfellow, J. Pouget-Abadie, M. Mirza, B. Xu, D. Warde-Farley, S. Ozair, A. Courville, and Y. Bengio. Generative adversarial nets. In *Advances in neural information processing systems*, pages 2672–2680, 2014.
- D. P. Kingma and M. Welling. Auto-encoding variational bayes. *International Conference on Learning Representations*, 2014.
- A. Makhzani, J. Shlens, N. Jaitly, I. Goodfellow, and B. Frey. Adversarial autoencoders. In *International Conference on Learning Representations*, 2016.
- S. Pidhorskyi, R. Almhosen, and G. Doretto. Generative probabilistic novelty detection with adversarial autoencoders. In *NIPS*, 2018.
- D. J. Rezende, S. Mohamed, and D. Wierstra. Stochastic backpropagation and approximate inference in deep generative models. In *International Conference on Machine Learning*, pages 1278–1286, 2014.
- S. Rifai, P. Vincent, X. Muller, X. Glorot, and Y. Bengio. Contractive auto-encoders: Explicit invariance during feature extraction. In *International Conference on Machine Learning*. Citeseer, 2011.
- M. Rosca, B. Lakshminarayanan, D. Warde-Farley, and S. Mohamed. Variational approaches for auto-encoding generative adversarial networks. In *arXiv preprint arXiv:1706.04987*, 2017.
- M. Rosca, B. Lakshminarayanan, and S. Mohamed. Distribution matching in variational inference. *arXiv preprint arXiv:1802.06847*, 2018.
- M. Sabokrou, M. Khalooei, M. Fathy, and E. Adeli. Adversarially learned one-class classifier for novelty detection. In *CVPR*, 2018.
- M. Sinn and A. Rawat. Non-parametric estimation of jensen-shannon divergence in generative adversarial network training. In *AISTATS*, 2018.
- L. Theis, A. v. d. Oord, and M. Bethge. A note on the evaluation of generative models. *arXiv preprint arXiv:1511.01844*, 2015.
- I. Tolstikhin, O. Bousquet, S. Gelly, and B. Schoelkopf. Wasserstein auto-encoders. *arXiv preprint arXiv:1711.01558*, 2017.
- M. Tschannen, O. Bachem, and M. Lucic. Recent advances in autoencoder-based representation learning. *arXiv preprint arXiv:1812.05069*, 2018.
- D. Ulyanov, A. Vedaldi, and V. Lempitsky. It takes (only) two: Adversarial generator-encoder networks. 2018.
- P. Vincent, H. Larochelle, Y. Bengio, and P.-A. Manzagol. Extracting and composing robust features with denoising autoencoders. In *Proceedings of the 25th international conference on Machine learning*, pages 1096–1103, 2008.
- Y. Wu, Y. Burda, R. Salakhutdinov, and R. Grosse. On the quantitative analysis of decoder-based generative models. *International Conference on Learning Representations (ICLR)*, 2017.
- Y. Xia, X. Cao, F. Wen, G. Hua, and J. Sun. Learning discriminative reconstructions for unsupervised outlier removal. In *ICCV*, 2015.
- Z. Xiao, Q. Yan, Y. Chen, and Y. Amit. Generative latent flow: A framework for non-adversarial image generation. *arXiv preprint arXiv:1905.10485*, 2019.
- J.-Y. Zhu, P. Krähenbühl, E. Shechtman, and A. A. Efros. Generative visual manipulation on the natural image manifold. In *European Conference on Computer Vision*, pages 597–613. Springer, 2016.

GENs: Generative Encoding Networks Supplementary Materials

1 Bandwidth estimation

1.1 Optimal bandwidth estimation for GENs

The KDE-based JSD loss, $\text{JSD}[p_e, p_t]$, between the encoded distribution, p_e , and target distribution, p_t , as defined in the main paper (leaving out the constants), is as follows:

$$\begin{aligned} \text{JSD}[p_e, p_t] = & \\ & \mathbb{E}_{\mathbf{z}' \sim p_e(\mathbf{z})} \left\{ \log \left[\frac{\frac{1}{m} \sum_{i=1}^m G_h(\mathbf{z}' - \mathbf{z}_i)}{p_t(\mathbf{z}') + \frac{1}{m} \sum_{i=1}^m G_h(\mathbf{z}' - \mathbf{z}_i)} \right] \right\} \\ & + \mathbb{E}_{\mathbf{z}'' \sim p_t(\mathbf{z})} \left\{ \log \left[\frac{p_t(\mathbf{z}'')}{p_t(\mathbf{z}'') + \frac{1}{m} \sum_{i=1}^m G_h(\mathbf{z}'' - \mathbf{z}_i)} \right] \right\} \end{aligned} \quad (1)$$

We require the derivative of $\text{JSD}[p_e, p_t]$, with respect to bandwidth, h , to determine the optimal bandwidth, h_{opt} , for a given latent dimension, l and KDE sample size, m . The derivative of $\text{JSD}[p_e, p_t]$, with respect to bandwidth, h , is as follows:

$$\begin{aligned} \frac{\partial \text{JSD}[p_e, p_t]}{\partial h} = & \mathbb{E}_{\mathbf{z}' \sim p_e(\mathbf{z})} \left(\frac{1}{h} \left[\frac{1}{\sum_{i=1}^m G_h(\mathbf{z}' - \mathbf{z}_i)} \right] \left[\sum_{i=1}^m G_h(\mathbf{z}' - \mathbf{z}_i) \frac{\|\mathbf{z}' - \mathbf{z}_i\|_2^2}{h^2} \right] - \frac{l}{h} \right) \\ & - \mathbb{E}_{\mathbf{z}' \sim p_e(\mathbf{z})} \left(\frac{1}{mh} \left[\frac{1}{p_t(\mathbf{z}') + \frac{1}{m} \sum_{i=1}^m G_h(\mathbf{z}' - \mathbf{z}_i)} \right] \left[\sum_{i=1}^m G_h(\mathbf{z}' - \mathbf{z}_i) \frac{\|\mathbf{z}' - \mathbf{z}_i\|_2^2}{h^2} \right] \right) \\ & + \mathbb{E}_{\mathbf{z}' \sim p_e(\mathbf{z})} \left(\left[\frac{\frac{1}{m} \sum_{i=1}^m G_h(\mathbf{z}' - \mathbf{z}_i)}{p_t(\mathbf{z}') + \frac{1}{m} \sum_{i=1}^m G_h(\mathbf{z}' - \mathbf{z}_i)} \right] \frac{l}{h} \right) \\ & - \mathbb{E}_{\mathbf{z}'' \sim p_t(\mathbf{z})} \left(\frac{1}{mh} \left[\frac{1}{p_t(\mathbf{z}'') + \frac{1}{m} \sum_{i=1}^m G_h(\mathbf{z}'' - \mathbf{z}_i)} \right] \left[\sum_{i=1}^m G_h(\mathbf{z}'' - \mathbf{z}_i) \frac{\|\mathbf{z}'' - \mathbf{z}_i\|_2^2}{h^2} \right] \right) \\ & + \mathbb{E}_{\mathbf{z}'' \sim p_t(\mathbf{z})} \left(\left[\frac{\frac{1}{m} \sum_{i=1}^m G_h(\mathbf{z}'' - \mathbf{z}_i)}{p_t(\mathbf{z}'') + \frac{1}{m} \sum_{i=1}^m G_h(\mathbf{z}'' - \mathbf{z}_i)} \right] \frac{l}{h} \right) \end{aligned} \quad (2)$$

The optimal bandwidth, h_{opt} , can be determined by either root trapping or fixed-point method using the derivative of $\text{JSD}[p_e, p_t]$ with respect to bandwidth, h . In our implementation, we have used root trapping method to determine h_{opt} . The solution for fixed-point update is derived in (3). Setting the derivative, $\frac{\partial \text{JSD}}{\partial h}$ in (2), to zero and multiplying both sides by h^3 , we get the fixed-point update as follows:

$$\begin{aligned} h^2 \leftarrow & F^{-1} \mathbb{E}_{\mathbf{z}' \sim p_e(\mathbf{z})} \left(\left[\frac{1}{\sum_{i=1}^m G_h(\mathbf{z}' - \mathbf{z}_i)} \right] \left[\sum_{i=1}^m G_h(\mathbf{z}' - \mathbf{z}_i) \|\mathbf{z}' - \mathbf{z}_i\|_2^2 \right] \right) \\ & - F^{-1} \mathbb{E}_{\mathbf{z}' \sim p_e(\mathbf{z})} \left(\frac{1}{m} \left[\frac{1}{p_t(\mathbf{z}') + \frac{1}{m} \sum_{i=1}^m G_h(\mathbf{z}' - \mathbf{z}_i)} \right] \left[\sum_{i=1}^m G_h(\mathbf{z}' - \mathbf{z}_i) \|\mathbf{z}' - \mathbf{z}_i\|_2^2 \right] \right) \\ & - F^{-1} \mathbb{E}_{\mathbf{z}'' \sim p_t(\mathbf{z})} \left(\frac{1}{m} \left[\frac{1}{p_t(\mathbf{z}'') + \frac{1}{m} \sum_{i=1}^m G_h(\mathbf{z}'' - \mathbf{z}_i)} \right] \left[\sum_{i=1}^m G_h(\mathbf{z}'' - \mathbf{z}_i) \|\mathbf{z}'' - \mathbf{z}_i\|_2^2 \right] \right) \end{aligned}$$

where, $F = l$

$$\begin{aligned}
 & - \mathbb{E}_{\mathbf{z}' \sim p_e(\mathbf{z})} \left(\left[\frac{\frac{1}{m} \sum_{i=1}^m G_h(\mathbf{z}' - \mathbf{z}_i)}{p_t(\mathbf{z}') + \frac{1}{m} \sum_{i=1}^m G_h(\mathbf{z}' - \mathbf{z}_i)} \right] l \right) \\
 & - \mathbb{E}_{\mathbf{z}'' \sim p_t(\mathbf{z})} \left(\left[\frac{\frac{1}{m} \sum_{i=1}^m G_h(\mathbf{z}'' - \mathbf{z}_i)}{p_t(\mathbf{z}'') + \frac{1}{m} \sum_{i=1}^m G_h(\mathbf{z}'' - \mathbf{z}_i)} \right] l \right)
 \end{aligned} \tag{3}$$

1.2 Optimal bandwidth estimation for entropy minimization

In the main paper, for target distribution, $p_t = \mathcal{N}(\mathbf{0}, \mathbf{I})$, we study how well-formed the Gaussian structure is in the latent space for different methods, after the autoencoder is optimized, by evaluating the entropy of the encoded distribution, p_e . The KDE based entropy using Gaussian kernels is defined as follows:

$$\mathbb{H}[p_e(\mathbf{z})] \approx -\frac{1}{m} \sum_i \log \frac{1}{m-1} \sum_{j \neq i} G_h(\mathbf{z} - \mathbf{z}_i), \tag{4}$$

In this experiment, the optimum bandwidth, h_{opt} , is determined using the derivative of $\mathbb{H}[p_e]$ with respect to h and solve for h_{opt} with a fixed point strategy, which gives the fixed point update as,

$$h^2 \leftarrow \frac{1}{lm} \sum_i \frac{\sum_{j \neq i} \|\mathbf{z}_j - \mathbf{z}_i\|_2^2 G_h(\mathbf{z}_j - \mathbf{z}_i)}{\sum_{j \neq i} G_h(\mathbf{z}_j - \mathbf{z}_i)}. \tag{5}$$

2 Results on bench-mark data

2.1 Reconstruction of test samples

Reconstruction of the held out samples of CelebA and SVHN data set for different methods are shown in Figure 1. These reconstructed samples are produced by the corresponding models used for estimating the FID scores reported in the main paper.

2.2 Generated samples

2.2.1 Standard Normal

In Figure 2, we present the generated samples using models trained over SVHN for different methods. The target distribution is standard normal for all the methods. The generated samples are produced by the corresponding models used for estimating the FID scores.

2.2.2 Mixture of Gaussians

Samples generated by interpolation in different modes of the mixture of Gaussians are reported in Figure 3. Generated samples corresponds to its mode in the distribution. These results validate the matching of the distribution in the latent space and clustering of the data (based on its labels) in the semi-supervised set up.

2.3 Novelty detection

Figure 4 shows the performance of the proposed outlier detection method, using models trained with GENs, on the held out data of the different category of digits in the MNIST data set.

2.4 Interpolation of the latent space

In this experiment, we linearly interpolate in the latent space between random samples in the latent space and projected test samples, for a model trained with GEN. In both the tests, we found the interpolated results to generate images bearing strong facial features for any pair of latent values. Figure 5 and 6 show generated images by linear interpolation of the random samples in the latent space and projected test samples in the latent space, respectively.



Figure 1: Reconstruction of held out data of CelebA (left) and SVHN (right) by (a) AAE (Makhzani et al., 2016) (b) VAE (Kingma and Welling, 2014) and (c) GEN (proposed). The size of the latent space for CelebA and SVHN are $l = 40$ and $l = 25$ respectively. Reconstruction of 64 test images of both data sets are shown in the figure for each method, where the reconstructed image follows the test input in the grid layout.

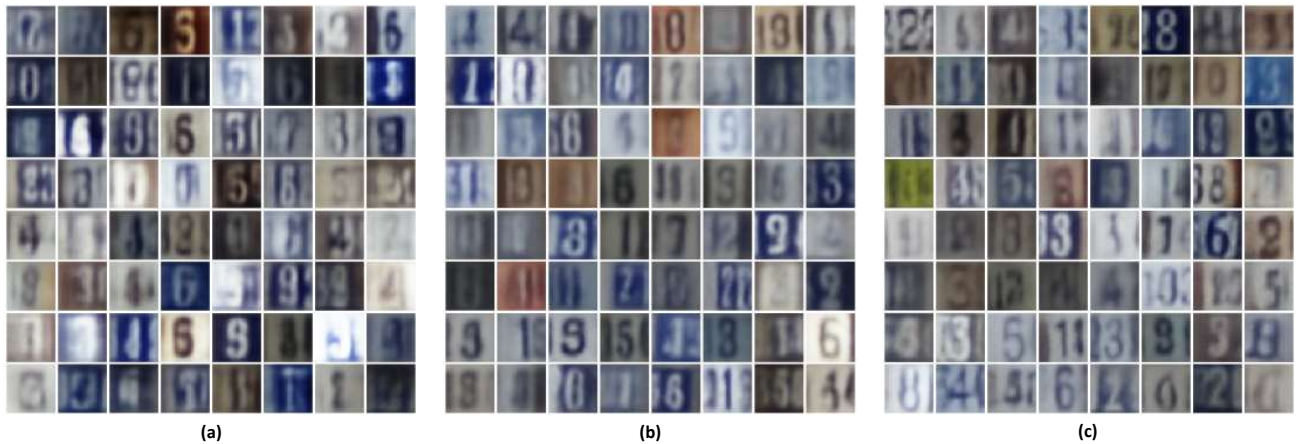


Figure 2: Samples generated by models trained with (a) AAE (Makhzani et al., 2016) (b) VAE (Kingma and Welling, 2014) and (c) GEN (proposed) over SVHN dataset in $l = 25$ dimensional latent space.

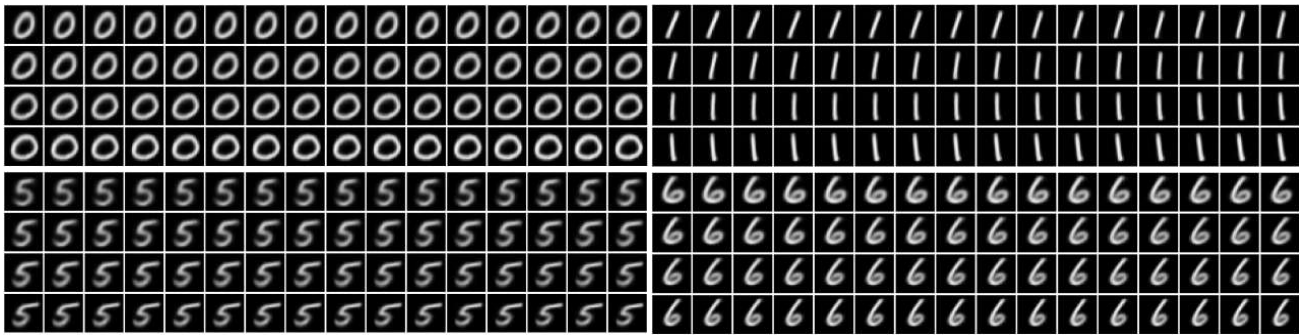


Figure 3: Samples generated by interpolation (along axes) in different modes of the mixture of Gaussians. The variation in the style of the generated samples is evident in all the modes.

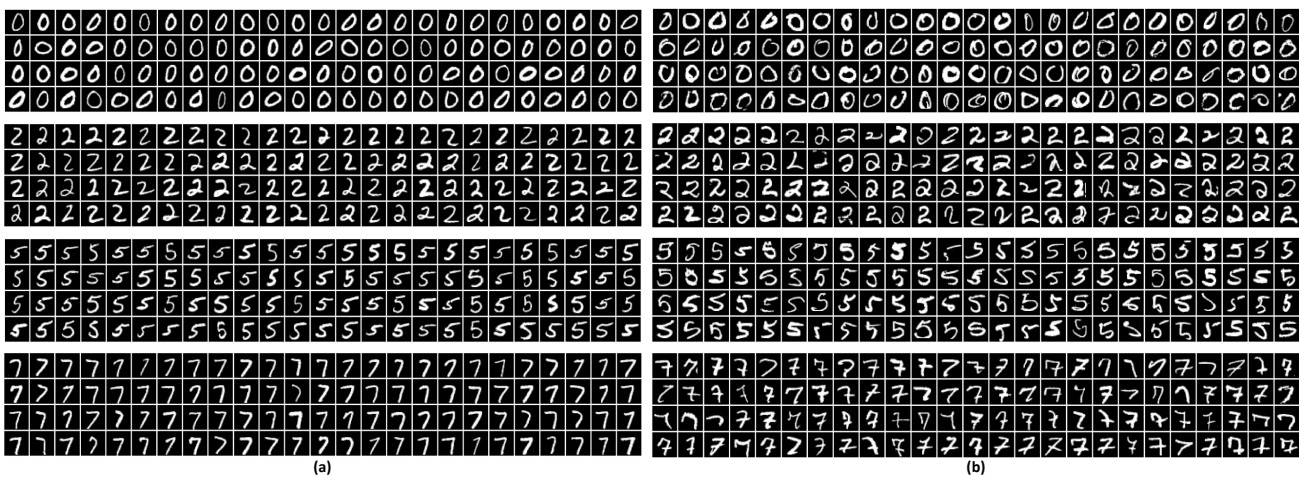


Figure 4: Novelty detection on the held out data of MNIST for digits 0, 2, 5, and 7 (a) 100 samples with low outlier score aka inliers and (b) 100 samples having high outlier score, identified as outliers to the distribution

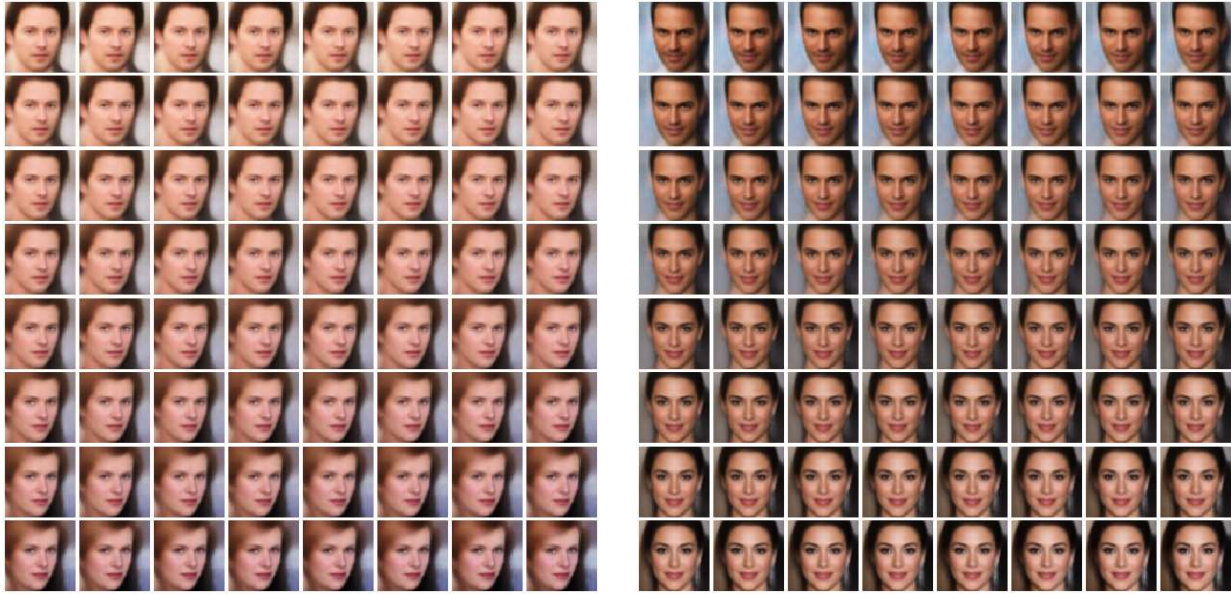


Figure 5: Images generated by interpolation between random pairs of samples in the latent space, for a model trained with GEN. The images at the left top and right bottom corners of the grid correspond to the images generated by the random pair of samples in the latent space. The interpolated results are shown across the columns in the grid, starting at the left top corner.

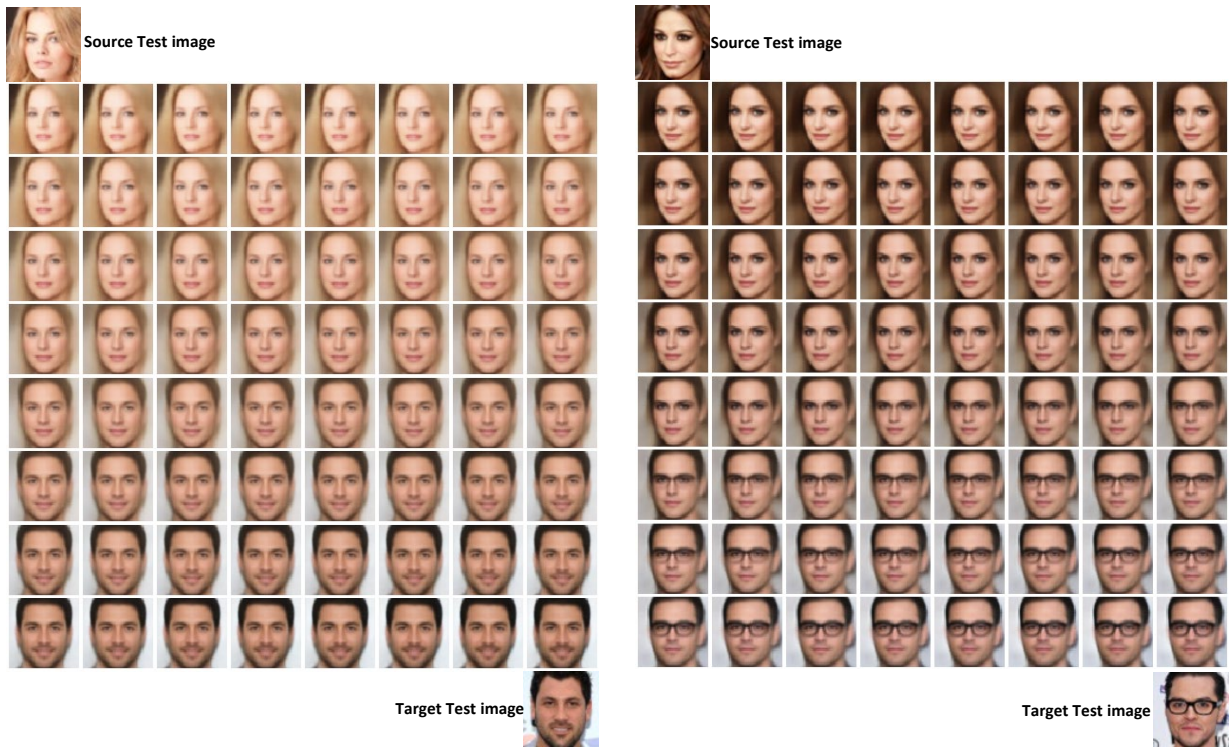


Figure 6: Images generated by interpolation between test images projected in the latent space, for a model trained with GEN. The real source and target test images are tagged along with the grid layout, showing interpolation results. We use the projection of the source and target image in the latent space, shown at the left top and right bottom corner of the grid respectively, for producing interpolation results. Images generated by interpolation are shown across the columns in the grid, starting at the left top corner.

References

- D. P. Kingma and M. Welling. Auto-encoding variational bayes. *International Conference on Learning Representations*, 2014.
- A. Makhzani, J. Shlens, N. Jaitly, I. Goodfellow, and B. Frey. Adversarial autoencoders. In *International Conference on Learning Representations*, 2016.